

PROCEEDINGS A

rspa.royalsocietypublishing.org

Research



Article submitted to journal

Subject Areas:

mathematical physics

Keywords:

spin-weighted spheroidal harmonics,
angular eigenvalues, black holes

Author for correspondence:

Niels Warburton

e-mail: niels.warburton@ucd.ie

High-order asymptotics for the Spin-Weighted Spheroidal Equation at large real frequency

Marc Casals^{1,2}, Adrian C. Ottewill² and
Niels Warburton²

¹Centro Brasileiro de Pesquisas Físicas (CBPF), Rio de Janeiro, CEP 22290-180, Brazil.

²School of Mathematics and Statistics, University College Dublin, Belfield, Dublin 4, Ireland.

The spin-weighted spheroidal eigenvalues and eigenfunctions arise in the separation by variables of spin-field perturbations of Kerr black holes. We derive a large, real-frequency asymptotic expansion of the spin-weighted spheroidal eigenvalues and eigenfunctions to high order. This expansion corrects and extends existing results in the literature and we validate it via a high-precision numerical calculation.

1. Introduction

Teukolsky derived a single “master” equation for spin-field perturbations of rotating (Kerr) black holes [1,2]. This $(3 + 1)$ -dimensional master equation separates by variables, with the polar-angular factor in the solution being the so-called spin-weighted spheroidal eigenfunction. The corresponding eigenvalue also appears in the equation satisfied by the radial factor of the Teukolsky master solution. Thus, both the eigenvalues and the eigenfunctions are important for studying perturbations of astrophysical black holes.

Neither the spin-weighted spheroidal eigenfunctions nor their eigenvalues are known in closed form but they can be calculated using numerical and analytical techniques (see [3,4] for a review). As for the analytical techniques, for example, expansions have been obtained for small frequency [5–8] and asymptotic analyses have been carried out for large, purely-imaginary frequency [3,4,9–11].

In this paper we are instead interested in the asymptotics for large, *real* frequency. These asymptotics are interesting for various reasons, such as for synchrotron radiation [9,12], for the study of divergences in either the quantum or classical field theories (e.g., [13,14] for WKB in the case of spherically-symmetric space-times and [15,16] for expressions for expectation values involving (spin-weighted) spheroidal harmonics in Kerr) and gravitational waves from rapidly rotating black holes [17,18]. Analytic approximations are also extremely valuable as checks on numerical calculation schemes. The large, real frequency behaviour of the *scalar* spheroidal eigenfunctions and eigenvalues was studied in [19–21]. The first large, real frequency study in the non-zero spin case was carried out in [9]. However, this work contained an error which was corrected by Breuer, Ryan and Waller [22] (BRW). BRW provided an asymptotic expansion for the eigenvalue up to six leading orders, which depended crucially on a parameter ${}_s q_{\ell m}$ that was left undetermined for the case of non-zero spin. Furthermore, their analysis for non-zero spin had an error in the asymptotic behaviour of the eigenfunctions which was later corrected in [23]. This correction further allowed [23] to analytically obtain the parameter ${}_s q_{\ell m}$ as well as the correct first term in a large real-frequency series expansion for the eigenfunctions.

As it turns out, however, the last three orders in the asymptotic expansion for the eigenvalue provided in BRW formally in terms of ${}_s q_{\ell m}$ were also incorrect. In this paper, we correct these 3rd-to-6th leading orders and extend the expansion up to four higher orders, thus providing the correct *ten* leading orders of the eigenvalue for large real frequency. We also provide the first few coefficients in the large, real-frequency expansion of the eigenfunctions, thus going, for the first time, beyond leading order. We compare our asymptotic expansions for both the eigenvalues and eigenfunctions with high-precision numerical calculations and find excellent agreement. The results of this paper together with those in [23] thus provide a correct, high-order asymptotic expansion of the eigenvalues and eigenfunctions for large, real frequency.

The layout of the rest of the paper is as follows. In Sec. 2 we introduce the spin-weighted spheroidal equation and its symmetries. In Sec. 3 we perform the large frequency asymptotic analysis of the spin-weighted spheroidal eigenfunctions and eigenvalues. We compare our asymptotic analysis and our numerical results in Sec. 4. In Appendix A we give explicit expressions for the coefficients in the series for the eigenfunctions and in Appendix B we describe the implementation of the asymptotics for the eigenvalue in a *Mathematica* toolkit.

2. Spin-Weighted Spheroidal Equation

Teukolsky [1,2] managed to decouple and separate by variables the linear spin-field perturbations of Kerr black holes. He achieved this for the radiative components of the massless fields of spin¹ $s = 0$ (scalar), $\pm 1/2$ (neutrino), ± 1 (electromagnetic) and ± 2 (gravitational). The polar-angular factors of the perturbations are the so-called spin-weighted spheroidal harmonics ${}_s S_{\ell m c}$. These

¹The symbol s really corresponds to the helicity of the spin-field, although in keeping with general convention, we refer to it as the spin.

functions satisfy the following linear, second-order ordinary differential equation (ODE):

$$\left(\frac{d}{dx}\left((1-x^2)\frac{d}{dx}\right) + c^2x^2 - 2scx - \frac{(m+sx)^2}{1-x^2} + {}_sE_{\ell mc} - s^2\right) {}_sS_{\ell mc}(x) = 0, \quad (2.1)$$

where $x \equiv \cos \theta \in [-1, +1]$ is the physical region of interest and $\theta \in [0, \pi]$ is the (Boyer-Lindquist) polar angle. Here, $c \equiv a\omega$, where $a \in \mathbb{R}$ is the angular momentum per unit mass of the black hole and $\omega \in \mathbb{C}$ is the frequency of the field mode. The multipole number $\ell = |s|, |s| + 1, |s| + 2, \dots$ serves to label the eigenvalue ${}_sE_{\ell mc}$ and $m = -\ell, -\ell + 1, \ell + 2, \dots, +\ell$ is the azimuthal number. The ODE (2.1) has two regular singular points at $x = \pm 1$ and an irregular singular point at $x = \infty$. The eigenvalue ${}_sE_{\ell mc}$ is chosen so that the corresponding solution ${}_sS_{\ell mc}$ is regular over $x \in [-1, +1]$. The case $s = 0$ yields the (scalar) spheroidal equation [19–21], whereas the case $c = 0$ yields the spin-weighted spherical equation [24] (in which case², ${}_sE_{\ell m 0} = \ell(\ell + 1)$).

Other common parameterizations of the eigenvalue are

$${}_s\lambda_{\ell mc} \equiv {}_sE_{\ell mc} - s(s+1) + c^2 - 2mc, \quad (2.2a)$$

$${}_sA_{\ell mc} \equiv {}_sE_{\ell mc} - s(s+1). \quad (2.2b)$$

The manifest symmetries of the spin-weighted spheroidal equation imply that

$$-{}_sS_{\ell mc}(x) = (-1)^{\ell+m} {}_sS_{\ell mc}(-x), \quad {}_sS_{\ell(-m)(-c)}(x) = (-1)^{\ell+s} {}_sS_{\ell mc}(-x), \quad (2.3)$$

where the choice of signs ensures consistency with the so-called Teukolsky-Starobinsky identities [25,26], and

$$-{}_sE_{\ell mc} = {}_sE_{\ell mc}, \quad {}_sE_{\ell m(-c)} = {}_sE_{\ell(-m)c}. \quad (2.4)$$

While ${}_s\lambda_{\ell mc}$ is most common in the current literature, we shall use ${}_sA_{\ell mc}$ in the following sections to ease comparison with BRW.

3. Large real-frequency asymptotics

In this paper we are interested in the large, real “frequency” (by which we really mean $c \rightarrow \pm\infty$) behaviour of the eigenvalues and eigenfunctions. In addition, by Eqs. (2.3) and (2.4) we may assume c positive and deduce the c negative behaviour from changing m to $-m$. We therefore restrict ourselves to $c > 0$ from now on.

We here generalize to arbitrary spin Flammer’s [20] approach in the scalar case – this is essentially BRW’s path, although they obtained some incorrect results which we specify and correct below. We start by writing solutions of the spin-weighted spheroidal equation (2.1) as

$${}_sS_{\ell mc}^{\pm}(x) = (1-x)^{|m+s|/2}(1+x)^{|m-s|/2}e^{-c(1\mp x)}g_{\pm}(x), \quad (3.1)$$

where $g_{\pm}(x)$ are regular functions. The powers of $(1-x)$ and $(1+x)$ are dictated by the Frobenius method, so that the solution is regular at both boundary points $x = +1$ and -1 . The exponential factor $e^{-c(1\mp x)}$ is included for convenience when looking for an asymptotic solution “near” $x = \pm 1$.

From Eq. (2.3), it follows that the solution $g_{-}(x)$ is obtained from $g_{+}(x)$ under the transformation $\{s \rightarrow -s, x \rightarrow -x\}$, modulo an overall sign of the solution. Hence, from now on we focus on g_{+} .

Looking for the asymptotic solution valid near $x = +1$, we introduce $u \equiv 2c(1-x)$. (For a full discussion see [23], where this procedure defines an asymptotic solution³ $S^{\text{inn},+1}(x)$ for $0 \leq 1-x \leq \mathcal{O}(c^{\delta})$ with $-1 < \delta < 0$.) Inserting the expression (3.1) into the ODE (2.1), we find that $g_{+}(u)$

²This corrects a typographical error in Eq. (1.3) [23].

³The function $S^{\text{inn},+1}(x)$ in [23] corresponds to the leading-order term in the expansion for g_{+} which we provide in this paper.

satisfies the following equation,

$$\begin{aligned} & ug_+'' + (|m+s|+1-u)g_+' + \frac{1}{2}(sq_{\ell m} - |m+s|-1-s)g_+ + \\ & {}_s\bar{A}_{\ell mc}g_+ - \frac{1}{4c}\left(u(ug_+'' + (|m+s|+|m-s|+2-u)g_+' + \right. \\ & \left. \frac{1}{2}((|m+s|+1)(|m-s|+1) - (m+1)^2 + s^2 - (|m+s|+|m-s|+2+2s)u)g_+)\right) = 0, \end{aligned} \quad (3.2)$$

where primes denote derivatives with respect to u . Here we have defined

$${}_s\bar{A}_{\ell mc} \equiv \frac{1}{4c} \left(s(s+1) - m(m+1) + c^2 - 2sq_{\ell m}c + {}_sA_{\ell mc} \right), \quad (3.3)$$

introducing the parameter $sq_{\ell m}$, discussed in the Introduction, which is chosen so that

$${}_s\bar{A}_{\ell mc} = o(1), \quad \text{as } c \rightarrow \infty. \quad (3.4)$$

BRW left the parameter $sq_{\ell m}$ undetermined for non-zero spin. Its value may be determined by requiring that the number of zeros of our asymptotic expansion⁴ is equal to the number of zeros of the spin-weighted spheroidal harmonics (which is given in Eq. (4.1) in Ref. [23]). Ref. [23] determined this value to be⁵

$$sq_{\ell m} = \ell + 1 - z_0, \quad \text{if } \ell \geq |s|\ell_m, \quad (3.5)$$

$$sq_{\ell m} = 2\ell + 1 - |s|\ell_m, \quad \text{if } \ell < |s|\ell_m, \quad (3.6)$$

where ${}_s\ell_m \equiv |m+s| + s$, and

$$z_0 \equiv \begin{cases} 0 & \text{if } \ell + m \text{ even,} \\ 1 & \text{if } \ell + m \text{ odd.} \end{cases} \quad (3.7)$$

The value of z_0 indicates whether ${}_sS_{\ell mc}(x)$ has a zero ‘‘near’’ $x=0$ for large- c : it is $z_0=1$ if ${}_sS_{\ell mc}(x)$ has a zero ‘‘near’’ $x=0$ and it is $z_0=0$ if it does not. Regarding the values of $sq_{\ell m}$, we note, in particular, that: (i) $sq_{\ell m}$ is an integer if s is an integer, whereas $sq_{\ell m}$ is a half-integer if s is a half-integer; (ii) $sq_{\ell m} = -sq_{\ell m}$.

In the limit of infinitely large c , only the first line in Eq. (3.2) survives and the solution of the resulting ODE which is regular at $u=0$ ($x=1$) is

$${}_1F_1(-{}_sp_{\ell m+}, |m+s|+1, u), \quad (3.8)$$

where we have introduced ${}_sp_{\ell m+} \equiv \frac{1}{2}(sq_{\ell m} - |m+s| - s - 1)$ and ${}_1F_1$ is the regular confluent hypergeometric function [19]. We note that ${}_sp_{\ell m+} \in \mathbb{Z}$ for $2s \in \mathbb{Z}$.

Eq. (3.2) then suggests that we express the function g_+ as

$$g_+(u) = \sum_{n=-\infty}^{\infty} a_n {}_1F_1(-{}_sp_{\ell m+} - n, |m+s|+1, u), \quad (3.9)$$

where without loss of generality we assume that $a_0 = 1$. The series coefficients a_n satisfy a three-term recurrence relation

$$\begin{aligned} & (2n + sq_{\ell m} - |m-s| + s + 1)(2n + sq_{\ell m} - |m+s| - s + 1)a_{n+1} + \\ & 2(8cn - (2n + sq_{\ell m})^2 + 2s^2 - (m+1)^2 - 8c{}_s\bar{A}_{\ell mc})a_n + \\ & (2n + sq_{\ell m} + |m-s| + s - 1)(2n + sq_{\ell m} + |m+s| - s - 1)a_{n-1} = 0. \end{aligned} \quad (3.10)$$

⁴Specifically, this number is obtained by adding the number of zeros of the leading order expression Eq. (3.8) near $x=+1$, the number of zeros of its counterpart near $x=-1$ and the number of zeros z_0 in Eq. (3.7) near $x=0$.

⁵It can be checked that our expressions for $sq_{\ell m}$ and z_0 here are equivalent to –but simpler than– those given in Eqs. (4.5) and (4.6) in [23].

These recurrence relations are obtained by inserting the series representation (3.9) into (3.2) and using the following recurrence relations satisfied by the hypergeometric functions [19]:

$$u {}_1F_1''(\alpha, \beta, u) + (\gamma - u) {}_1F_1'(\alpha, \beta, u) = (\gamma - \beta) {}_1F_1'(\alpha, \beta, u) + \alpha {}_1F_1(\alpha, \beta, u), \quad (3.11a)$$

$$u {}_1F_1'(\alpha, \beta, u) = \alpha ({}_1F_1(\alpha + 1, \beta, u) - {}_1F_1(\alpha, \beta, u)), \quad (3.11b)$$

$$u {}_1F_1(\alpha, \beta, u) = \alpha {}_1F_1(\alpha + 1, \beta, u) - (2\alpha - \beta) {}_1F_1(\alpha, \beta, u) + (\alpha - \beta) {}_1F_1(\alpha - 1, \beta, u), \quad (3.11c)$$

for constant α , β and γ . Because of the analyticity of the coefficients of the spin-weighted spheroidal differential equation in the parameter c , we can assume a series expansion in powers of $1/c$ for ${}_s\bar{A}_{\ell mc}$ (see, e.g., theorems 2.9 and 4.9 in Ch. 8 in Ref. [27]):

$${}_s\bar{A}_{\ell mc} \sim \sum_{k=1}^{\infty} \bar{A}_k c^{-k} \quad \text{as } c \rightarrow \infty. \quad (3.12)$$

Correspondingly we now expand the coefficients for large- c :

$$a_n \sim \sum_{k=|n|}^{\infty} a_{n,k} c^{-k} \quad \text{as } c \rightarrow \infty, \quad (3.13)$$

where the structure of this coefficient expansion follows from the dominant first term in the coefficient of a_n in the recurrence relation. We give explicit expressions for the series coefficients $a_{n,k}$ for $n : -3 \rightarrow 3$ and $k : |n| \rightarrow 3$ in Appendix A.

Inserting the expansions Eqs. (3.12) and (3.13) into the recurrence relation (3.10) and requiring it to be satisfied order-by-order determines the expansion coefficients. Specifically, we find ${}_sA_{\ell mc}$ takes the form

$${}_sA_{\ell mc} = -c^2 + 2{}_sq_{\ell m}c - \frac{1}{2} ({}_sq_{\ell m}^2 - m^2 + 2s + 1) + \sum_{k=1}^7 \frac{A_k}{c^k} + O\left(\frac{1}{c^8}\right). \quad (3.14)$$

Other common definitions of the eigenvalue are easily computed from this using Eqs. (2.2a) and (2.2b). Dropping the subscripts on ${}_sq_{\ell m}$ for compactness, the A_k 's are given by

$$A_1 = -\frac{1}{8} (q^3 - m^2q + q - 2s^2(q + m)), \quad (3.15)$$

$$A_2 = \frac{1}{64} (-m^4 + 6m^2q^2 + 2m^2 - 5q^4 - 10q^2 - 1 + 4s^2(m^2 + 4mq + 3q^2 + 1)), \quad (3.16)$$

$$A_3 = \frac{1}{512} (-q(37 + 13m^4 + 114q^2 + 33q^4 - 2m^2(25 + 23q^2)) + 4(13m - m^3 + 25q + 9m^2q + 33mq^2 + 23q^3)s^2 - 8(m + q)s^4), \quad (3.17)$$

$$A_4 = \frac{1}{1024} (-14 + 2m^6 - 239q^2 - 340q^4 - 63q^6 - 3m^4(6 + 13q^2) + 10m^2(3 + 23q^2 + 10q^4) + 4(-m^4 - 9m^3q + 5m^2(2 + 3q^2) + mq(93 + 73q^2) + 5(3 + 23q^2 + 10q^4))s^2 - 8(2 + 3m^2 + 9mq + 6q^2)s^4), \quad (3.18)$$

$$A_5 = \frac{1}{8192} (-q(1009 - 53m^6 + 5221q^2 + 4139q^4 + 527q^6 + 5m^4(127 + 93q^2) - m^2(1591 + 3750q^2 + 939q^4)) + 2(14m^5 - 45m^4q + 130m^2q(3 + q^2) - 20m^3(7 + 18q^2) + 2m(303 + 1820q^2 + 685q^4) + q(1591 + 3750q^2 + 939q^4))s^2 - 80(7m + m^3 + 11q + 9m^2q + 18mq^2 + 10q^3)s^4 + 16(m + q)s^6), \quad (3.19)$$

$$\begin{aligned}
A_6 = \frac{1}{131072} & \left(-3747 - 51m^8 - 86940q^2 - 205898q^4 - 101836q^6 - 9387q^8 + 12m^6(85 + 167q^2) - \right. \\
& 6m^4(939 + 5078q^2 + 1855q^4) + 12m^2(701 + 8657q^2 + 9575q^4 + 1547q^6) + \\
& 8(19m^6 + 270m^5q - m^4(191 + 309q^2) - 4m^3q(919 + 725q^2) + m^2(949 + 1482q^2 - 255q^4) + \\
& 2mq(8135 + 15310q^2 + 3363q^4) + 3(701 + 8657q^2 + 9575q^4 + 1547q^6))s^2 + \\
& 16(-467 + 17m^4 - 236m^3q - 3438q^2 - 1455q^4 - 4mq(919 + 725q^2) - 2m^2(407 + 849q^2))s^4 + \\
& \left. 128(4 + 7m^2 + 19mq + 12q^2)s^6 \right). \tag{3.20}
\end{aligned}$$

$$\begin{aligned}
A_7 = \frac{1}{2097152} & \left(-q(822221 + 4093m^8 + 5771940q^2 + 7568470q^4 + 2520820q^6 + 175045q^8) - \right. \\
& 1540m^6(65 + 43q^2) + 42m^4(16371 + 29350q^2 + 6375q^4) - \\
& 4m^2(353449 + 1345421q^2 + 847819q^4 + 95167q^6) - \\
& 8(257m^7 - 1253m^6q + 35m^4q(379 + 169q^2) - 35m^5(181 + 381q^2) + \\
& 7m^2q(-6821 + 6070q^2 + 3567q^4) + \\
& 7m^3(5389 + 32190q^2 + 12045q^4) - q(353449 + 1345421q^2 + 847819q^4 + 95167q^6) - \\
& m(112285 + 1057707q^2 + 953715q^4 + 136773q^6))s^2 + \\
& 112(31m^5 + 363m^4q - 6m^3(107 + 131q^2) - \\
& 10m^2q(1135 + 749q^2) - q(10573 + 23530q^2 + 5673q^4) - m(5389 + 32190q^2 + 12045q^4))s^4 + \\
& \left. 896(73m + 19m^3 + 105q + 113m^2q + 189mq^2 + 95q^3)s^6 - 640(m + q)s^8 \right). \tag{3.21}
\end{aligned}$$

While for compactness we have given just the first ten orders (to order $1/c^7$) for ${}_sA_{\ell mc}$ in Eq. (3.14), the process is easy to automate as it is for the a_n 's. We have implemented code into the `SpinWeightedSpheroidalHarmonics` package of the Black Hole Perturbation Toolkit to compute the high-frequency expansion of the eigenvalue – see Appendix B. We also provide additional code to compute the $a_{n,k}$'s and A_k 's to arbitrary order.

We note that BRW gave an expansion for ${}_sA_{\ell mc}$ to the first six orders (i.e., to order $1/c^3$) but, while their first three orders were as in Eq. (3.14), our values of A_1 , A_2 and A_3 correct the corresponding last three orders in Eq. (4.12) in BRW⁶. We also note that for $s = 0$ our results for the A_k 's agree with Ref. [28]. Finally, we note that it could also be interesting to consider the limit where both $c \rightarrow \infty$ and $m \rightarrow \infty$ with a fixed m/c ratio. This has been analysed in the $s = 0$ case [29] but has not, to the best of our knowledge, been analysed in the $s \neq 0$ case. We leave such an analysis for future work.

4. Comparison with numerical calculation

We validate our high-frequency asymptotic expansions by comparing them against a numerical calculation. For the numerical results we use the `SpinWeightedSpheroidalHarmonics` *Mathematica* package which is part of the Black Hole Perturbation Toolkit [30]. This package employs both a spectral method [31] and Leaver's method [32,33], combining them in a similar fashion to the method used by Ref. [34] for the $s = 0$ case, to rapidly compute high precision values for the spin-weighted spheroidal-harmonics and their eigenvalues.

For the eigenvalue calculation we use the `SpinWeightedSpheroidalEigenvalue` to compare against Eq. (3.14). Note that Eq. (3.14) gives the expansion for ${}_sA_{\ell mc}$, whereas the `SpinWeightedSpheroidalEigenvalue` command returns ${}_s\lambda_{\ell mc}$ so we use Eqs. (2.2a) and

⁶Eq. (4.12) in BRW was merely reproduced in [23] and in [3] without previously checking it, and so containing the last three erroneous terms of the original BRW version.

(2.2b) to convert between them. The results of the comparison are shown in Fig. 1 which shows that our high-frequency expansion agrees extremely well with the numerical results for large c . The comparison is further discussed in the figure's caption.

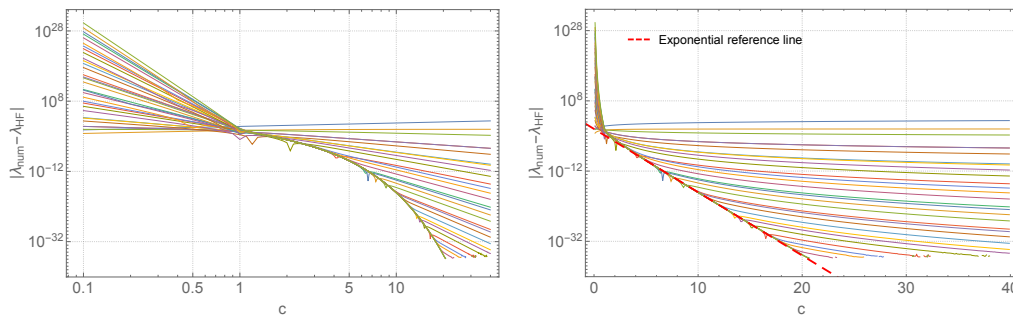


Figure 1. Difference between the numerically computed eigenvalue, λ_{num} , (computed to 40-digits of accuracy) and its high-frequency expansion, λ_{HF} , for the case $\{s, \ell, m\} = \{2, 2, 2\}$. We present the same results on both a log-log scale (left panel) and a log scale (right panel). The different curves are computed using successively higher orders in the high frequency expansion. On the right of the graph, the top curve plots the numerical value of the eigenvalue. The subsequent lower curves are computed by subtracting the high-frequency series truncated at $\mathcal{O}(c^1)$, $\mathcal{O}(c^0)$, $\mathcal{O}(c^{-1}) \dots \mathcal{O}(c^{-27})$, respectively. For $c \gtrsim 1$ including additional terms in the high frequency series improves the comparison with the numerical results up to a point. After this, adding more terms does not improve the agreement. The shape of the curve beyond which adding terms not does improve the agreement is clearest on a log scale (right panel). This suggests that in addition to admitting a series expansion in c^{-1} there is an exponential term which the power law expansion cannot capture. Finally, as one would expect of a high frequency expansion, for $c \lesssim 1$ adding terms acts to worsen the agreement with the numerical results. The eigenvalue is better approximated by small frequency expansions around $c = 0$ in this region.

For the numerical calculation of the eigenfunctions we use the `SpinWeightedSpheroidalHarmonicS` command which computes ${}_s S_{\ell m c} e^{im\varphi}$ in our notation. These harmonics are normalized such that

$$\int_0^{2\pi} \int_0^\pi {}_s S_{\ell_1 m_1 c}(\theta) e^{im_1 \varphi} {}_s S_{\ell_2 m_2 c}(\theta) e^{-im_2 \varphi} \sin \theta d\theta d\varphi = \delta_{\ell_1}^{\ell_2} \delta_{m_1}^{m_2}, \quad (4.1)$$

where δ is the Kronecker delta function. On the other hand, we do not know the normalization of the ${}_s S_{\ell m c}^\pm$ in Eq. (3.1) with the g_\pm given by (3.9) and its $\{s \rightarrow -s, x \rightarrow -x\}$ counterpart. To make a meaningful comparison with the numerical calculation of the harmonics we numerically integrate ${}_s S_{\ell m c}^+$ over $x \in [1, 0]$, and ${}_s S_{\ell m c}^-$ over $x \in [0, -1]$ to obtain their normalization. With this information we can ensure that the numerical and asymptotic approximate solutions are normalized the same. Figure 2 presents an example of the excellent agreement we find between the numerical calculation and the high-frequency approximation of the eigenfunctions. The convergence of the expansion in Eq. (3.9) becomes slower the further the point is from $x = +1$; similarly for g_- from $x = -1$. This means that the combined asymptotic expansion of ${}_s S_{\ell m c}^+$ and ${}_s S_{\ell m c}^-$ converges more slowly near $x=0$, as reflected in Fig. 2. The convergence near $x = 0$ could be improved by incorporating the ‘outer’ solution of Eq. (3.26) in Ref. [23] in the manner done in Sec. III. C of that paper.

For the eigenvalues and the eigenfunctions, the excellent agreement we observe between the high-frequency asymptotics and the numerical results gives us confidence in both.

Data Accessibility. Code to compute the expansions in this paper to arbitrary order has been integrated into the open source Black Hole Perturbation Toolkit (bhptoolkit.org) – see Appendix B for more details.

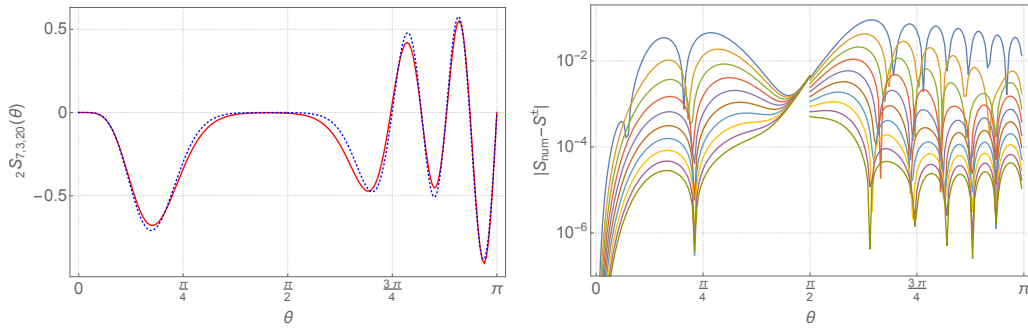


Figure 2. Example of the high-frequency approximation to the spheroidal-harmonic eigenfunction for parameters $\{s, \ell, m, c\} = \{2, 7, 3, 20\}$. (Left panel) The (red) solid curve shows the numerically computed value of ${}_2S_{7,3,20}$. The leading-order approximation is shown with the (blue) dotted curve. (Right panel) Including higher-order terms in the expansion improves the agreement with the numerical results. In this figure the top curve is the difference between the leading-order expansion and the numerical data. Successive lower curves are the difference between the numerical expansion and successively higher-order expansions.

Authors' Contributions. MC and ACO calculated the high-order large-frequency expansions presented in this work. NW made detailed comparisons of these expansions with high-precision numerical calculations and integrated all three authors' codes into the Black Hole Perturbation Toolkit.

Competing Interests. We have no competing interests.

Ethics. There are no ethical concerns regarding this work.

Funding. MC acknowledges partial financial support by CNPq (Brazil), process number 310200/2017-2. NW gratefully acknowledges support from a Royal Society - Science Foundation Ireland University Research Fellowship.

Acknowledgements. This work makes use of the Black Hole Perturbation Toolkit.

A. Eigenfunction coefficients

For completeness we here give the first three orders for the coefficients in the eigenfunction asymptotic expansion – see Eqs.(3.9) and (3.13). The coefficients $a_{n,k}$ may conveniently be expressed in terms of ${}_s p \ell m_{\pm} \equiv \frac{1}{2}(s q \ell m - |m \pm s| \mp s - 1)$, again dropping the subscripts on ${}_s p \ell m_{\pm}$ and ${}_s q \ell m$ for compactness:

$$a_{-1,1} = \frac{1}{4} p_- p_+, \quad (\text{A } 1a)$$

$$a_{1,1} = -\frac{1}{4} (p_- - q - s)(p_+ - q + s), \quad (\text{A } 1b)$$

$$a_{-2,2} = \frac{1}{32} p_- (p_- - 1) p_+ (p_+ - 1), \quad (\text{A } 2a)$$

$$a_{-1,2} = \frac{1}{8} p_- p_+ (q - 1), \quad (\text{A } 2b)$$

$$a_{1,2} = -\frac{1}{8} (p_- - q - s)(p_+ - q + s)(q + 1), \quad (\text{A } 2c)$$

$$a_{2,2} = \frac{1}{32} (p_- - q - s)(p_- - q - s - 1)(p_+ - q + s)(p_+ - q + s - 1), \quad (\text{A } 2d)$$

$$a_{-3,3} = \frac{1}{384} p_- (p_- - 1)(p_- - 2) p_+ (p_+ - 1)(p_+ - 2), \quad (\text{A } 3a)$$

$$a_{-2,3} = \frac{1}{64} p_- (p_- - 1) p_+ (p_+ - 1)(2q - 3), \quad (\text{A } 3b)$$

$$a_{-1,3} = \frac{1}{128} p_- p_+ ((p_- (p_- - q - s + 1) - q - s - 2) \times \\ (p_+ (p_+ - q + s + 1) - q + s - 2) + 2(q - 2)(5q - 2) - 2s^2), \quad (\text{A } 3c)$$

$$a_{1,3} = \frac{1}{128} (p_- - q - s)(p_+ - q + s) \times \\ ((p_- (p_- - q - s + 1) - 2)(p_+ (p_+ - q + s + 1) - 2) + 2(q + 2)(5q + 2) - 2s^2), \quad (\text{A } 3d)$$

$$a_{2,3} = \frac{1}{64} (p_- - q - s)(p_- - q - s - 1)(p_+ - q + s)(p_+ - q + s - 1)(2q + 3), \quad (\text{A } 3e)$$

$$a_{3,3} = -\frac{1}{384} (p_- - q - s)(p_- - q - s - 1)(p_- - q - s - 2)(p_+ - q + s) \times \\ (p_+ - q + s - 1)(p_+ - q + s - 2). \quad (\text{A } 3f)$$

These series coefficients were not given in BRW or, to the best of our knowledge, anywhere else in the literature.

As noted in the body of the paper, it is ${}_s p_{\ell m} \in \mathbb{Z}$ for $2s \in \mathbb{Z}$, and it is straightforward to show that ${}_s p_{\ell m} \geq 0$ for $s \geq 0$ and ${}_s p_{\ell m} \geq 0$ for $s \leq 0$. The structure of the expanded recursion relations then shows that the functional expansion Eq. (3.9) terminates with finite lower limit “ $-{}_s p_{\ell m}$ ” for $s \geq 0$, reflected in the vanishing of the coefficients $a_{n,k}$ for $n < -{}_s p_{\ell m}$. Corresponding comments hold for $s \leq 0$ with ${}_s p_{\ell m}$ replaced by ${}_s p_{\ell m}$. For $s = 0$, ${}_0 p_{\ell m} = {}_0 p_{\ell m}$ and our observation agrees with Eq. (8.2.9) of Flammer [20].

B. Implementation in the Black Hole Perturbation Toolkit

We have implemented the calculation of the high frequency expansion of the spin-weighted spheroidal eigenvalue and eigenfunction into the *Mathematica* SpinWeightedSpheroidalHarmonics package which is part of the open-source Black Hole Perturbation Toolkit. This package allows for the numerical and (where possible) analytic calculation of the eigenvalue and eigenfunction of the spin-weighted spheroidal equation. It also allows the user to compute small frequency expansions of these functions using the standard *Mathematica* Series[...] function. Following this work, we have implemented the high (real) frequency expansion of the eigenfunction as well.

As an example, the high-frequency expansion of the eigenvalue, ${}_s \lambda_{\ell m c}$, for $\{s, \ell, m\} = \{2, 7, 3\}$ about $c = \infty$ can be computed via

$$\text{Series}[\text{SpinWeightedSpheroidalEigenvalue}[2, 7, 3, c], \{c, \infty, 5\}] = \\ 10c - 30 - \frac{45}{c} - \frac{405}{2c^2} - \frac{9855}{8c^3} - \frac{17685}{2c^4} - \frac{2261115}{32c^5} + \mathcal{O}[c^{-6}] \quad (\text{A } 1)$$

The expansion can also be computed around $c = -\infty$, for example:

$$\text{Series}[\text{SpinWeightedSpheroidalEigenvalue}[2, 7, 3, -c], \{c, \infty, 5\}] = \\ 22c - 30 - \frac{51}{c} - \frac{501}{2c^2} - \frac{13017}{8c^3} - \frac{24603}{2c^4} - \frac{3283149}{32c^5} + \mathcal{O}[c^{-6}] \quad (\text{A } 2)$$

We have also included an example notebook in the Toolkit which demonstrates the use of this function and provides code to calculate the $a_{n,k}$ and A_k coefficients that appear in Eq. (3.13) and Eq. (3.14), respectively.

References

1. Teukolsky SA. 1972 Rotating black holes: Separable wave equations for gravitational and electromagnetic perturbations. *Physical Review Letters* **29**, 1114.
2. Teukolsky SA. 1973 Perturbations of a rotating black hole. 1. Fundamental equations for gravitational, electromagnetic and neutrino-field perturbations. *Astrophys. J.* **185**, 635–647.

3. Berti E, Cardoso V, Casals M. 2006a Eigenvalues and eigenfunctions of spin-weighted spheroidal harmonics in four and higher dimensions. *Phys. Rev.* **D73**, 024013.
4. Berti E, Cardoso V, Casals M. 2006b Erratum: Eigenvalues and eigenfunctions of spin-weighted spheroidal harmonics in four and higher dimensions [Phys. Rev. D 73, 024013 (2006)]. *Physical Review D* **73**, 109902.
5. Press WH, Teukolsky SA. 1973 Perturbations of a rotating black hole. II. Dynamical stability of the Kerr metric. *The Astrophysical Journal* **185**, 649–674.
6. Starobinskii AA, Churilov SM. 1974 Amplification of electromagnetic and gravitational waves scattered by a rotating "black hole". *Sov. Phys. JETP* **65**, 1–5.
7. Fackerell ED, Crossman RG. 1977 Spin-weighted angular spheroidal functions. *Journal of Mathematical Physics* **18**, 1849–1854.
8. Seidel E. 1989 A comment on the eigenvalues of spin-weighted spheroidal functions. *Classical and Quantum Gravity* **6**, 1057.
9. Breuer RA. 1975 Gravitational perturbation theory and synchrotron radiation. In *Lecture Notes in Physics, Berlin Springer Verlag* vol. 44.
10. Berti E, Cardoso V, Yoshida S. 2004 Highly damped quasinormal modes of Kerr black holes: A Complete numerical investigation. *Phys. Rev.* **D69**, 124018.
11. Hod S. 2013 Black-hole perturbation theory: The asymptotic spectrum of the prolate spin-weighted spheroidal harmonics. *Phys. Rev.* **D87**, 064017.
12. Chrzanowski PL, Misner CW. 1974 Geodesic synchrotron radiation in the Kerr geometry by the method of asymptotically factorized Green's functions. *Physical Review D* **10**, 1701.
13. Casals M, Dolan S, Ottewill AC, Wardell B. 2009 Padé Approximants of the Green Function in Spherically Symmetric Spacetimes. *Phys. Rev.* **D79**, 124044.
14. Anderson PR, Hiscock WA, Samuel DA. 1995 Stress-energy tensor of quantized scalar fields in static spherically symmetric spacetimes. *Phys. Rev. D* **51**, 4337–4358.
15. Ottewill AC, Winstanley E. 2000 The renormalized stress tensor in Kerr space-time: General results. *Phys. Rev.* **D62**, 084018.
16. Casals M, Ottewill AC. 2005 Canonical quantization of the electromagnetic field on the Kerr background. *Phys. Rev.* **D71**, 124016.
17. Yang H, Zimmerman A, Zenginoğlu A, Zhang F, Berti E, Chen Y. 2013 Quasinormal modes of nearly extremal Kerr spacetimes: spectrum bifurcation and power-law ringdown. *Phys. Rev.* **D88**, 044047.
18. Gralla SE, Porfyriadis AP, Warburton N. 2015 Particle on the Innermost Stable Circular Orbit of a Rapidly Spinning Black Hole. *Phys. Rev.* **D92**, 064029.
19. Erdelyi A, Magnus W, Oberhettinger F, Tricomi F. 1953 *Higher Transcendental Functions*. New York: McGraw-Hill.
20. Flammer C. 1957 *Spheroidal Wave Functions*. Stanford: Stanford University Press.
21. Meixner J, Schäfer FW. 2013 *Mathieusche Funktionen und Sphäroidfunktionen: mit Anwendungen auf physikalische und technische Probleme* vol. 71. Springer-Verlag.
22. Breuer RA, Ryan MP, Waller S. 1977 Some properties of spin-weighted spheroidal harmonics. *Proc. R. Soc. Lond. A* **358**, 71–86.
23. Casals M, Ottewill AC. 2005 High Frequency Asymptotics for the Spin-Weighted Spheroidal Equation. *Phys. Rev.* **D71**, 064025.
24. Goldberg J, Macfarlane A, Newman ET, Rohrlich F, Sudarshan E. 1967 Spin-s Spherical Harmonics and δ . *Journal of Mathematical Physics* **8**, 2155–2161.
25. Teukolsky SA, Press W. 1974 Perturbations of a rotating black hole. III-Interaction of the hole with gravitational and electromagnetic radiation. *The Astrophysical Journal* **193**, 443–461.
26. Chandrasekhar S. 1983 *The Mathematical Theory of Black Holes*. New York: Oxford University Press.
27. Kato T. 1966 *Perturbation theory for linear operators, volume 132 of Grundlehren der mathematischen Wissenschaften*. Springer-Verlag, Berlin.
28. Do-Nhat T. 2001 Asymptotic expansions of the oblate spheroidal eigenvalues and wave functions for large parameter c . *Canadian Journal of Physics* **79**, 813–831.
29. Hod S. 2015 Eigenvalue spectrum of the spheroidal harmonics: A uniform asymptotic analysis. *Phys. Lett.* **B746**, 365–367.
30. Black Hole Perturbation Toolkit. (bhptoolkit.org).
31. Hughes SA. 2000 The Evolution of circular, nonequatorial orbits of Kerr black holes due to gravitational wave emission. *Phys. Rev.* **D61**, 084004.

32. Leaver EW. 1985 An Analytic Representation for the Quasi-Normal Modes of Kerr Black Holes. *Proc. Roy. Soc. Lond. A* **402**, 285.
33. Leaver EW. 1986 Solutions to a generalized spheroidal wave equation: Teukolsky's equations in general relativity, and the two-center problem in molecular quantum mechanics. *J. Math. Phys.* **27**, 1238.
34. Falloon PE, Abbott PC, Wang JB. 2003 Theory and computation of spheroidal wavefunctions. *Journal of Physics A Mathematical General* **36**, 5477–5495.